Engineering the chromatic dispersion in dual-wavelength metalenses for unpolarized visible light

Zi-Hang Huo, Xiao-Ning Pang, Hong Wang, Zhi-Bin Fan, Xiang-Yang Yu, et al.

Zi-Hang Huo, Xiao-Ning Pang, Hong Wang, Zhi-Bin Fan, Xiang-Yang Yu, Jian-Wen Dong, Shao-Ji Jiang, "Engineering the chromatic dispersion in dual-wavelength metalenses for unpolarized visible light," Proc. SPIE 11170, 14th National Conference on Laser Technology and Optoelectronics (LTO 2019), 111702H (17 May 2019); doi: 10.1117/12.2533715

Event: Fourteenth National Conference on Laser Technology and Optoelectronics, 2019, Shanghai, China

Engineering the chromatic dispersion in dual-wavelength metalenses for unpolarized visible light

Zi-Hang Huo[a,b,#], Xiao-Ning Pang[a,c,#], Hong Wang[*a,c], Zhi-Bin Fan[a,c], Xiang-Yang Yu[a,c], Jian-Wen Dong[a,c], Shao-Ji Jiang[a,c]
[a]State Key Laboratory of Optoelectronic Materials and Technologies, Sun Yat-sen University, Guangzhou 510275, China;
[b]School of Electronics and Information Technology, Sun Yat-sen University, Guangzhou 510275, China;
[c]School of Physics, Sun Yat-sen University, Guangzhou 510275, China

ABSTRACT

Chromatic dispersion represents the wavelength-dependent behavior of optical devices and limits their operation bandwidth. Due to the material dispersion restriction of refractive elements, dispersion engineering remains a challenge to imaging technology and optical communication. Recently, metalens offers an attractive approach to engineer the dispersion by introducing the additional degree of freedom with only a single layer of nanostructures. Here, we propose a method to design the dual-wavelength metalenses with controllable dispersion characteristic in transmission mode in the visible region. Three kinds of polarization-independent metalenses are demonstrated, including those with zero dispersion, positive axial dispersion, and negative axial dispersion. All the metalenses show high resolution with nearly diffraction-limited focusing. Our findings may provide an alternative way to design dual-wavelength functional devices in the fields of optical information processing, imaging technologies and complex fluorescence techniques.

Keywords: Dual-wavelength, controllable dispersion, unpolarized light, metalenses

1. INTRODUCTION

Chromatic dispersion is an inherent phenomenon that the electromagnetic wave propagating speed depends on the frequency and material. Chromatic dispersion of a certain device refers to the derivative of its given performance parameter with respect to the frequency. For the optical lens, chromatic dispersion reflects the variation of focus with the frequency or wavelength. Different dispersion is beneficial to different specific applications, such as spectrometers [1], superprisms [2], and slow light devices [3]. Therefore, to engineer the optical lens with delicate dispersion is extremely attractive in the fields of imaging and optical communication. In conventional refractive optics, numerous efforts have been made to develop the optical lenses [4, 5] with certain dispersion. The achromatic doublet and apochromatic triplet have been used to correct the chromatic aberration at two and three wavelengths [6], respectively. The adoption of the unsymmetrical freeform optics with arbitrary shape offers new opportunities in eliminating or expanding the dispersion [7]. However, the conventional lenses require two or more components and thus bulky sizes to engineer the dispersion, which is hard to apply to the wearable and portable devices. The additional components will also bring stricter challenge to the manufacturing processing and alignment technique. Hence, a planar, single optical element is rather in need to engineer the chromatic dispersion arbitrarily.

Recently, metasurfaces draw extensive attention with their enhanced functionalities and planar features [8-10], and provide an alternative platform to achieve the chromatic dispersion. By arranging the array of nanostructures intelligently, metasurfaces have proven capable of implementing many planar devices, including beam deflectors [11, 12], vortex beam generators [12, 13], holograms [14, 15], vector beam generators [16], and especially the metalenses [17, 18]. Metalenses have been proved to engineer the dispersion with exceeding performance. For instance, strong dispersion was observed when the metalenses operate in off-axis, and thus compact spectrometers have been demonstrated in both visible [19] and the near infrared regions [20] with unprecedented spectral resolution. Besides, zero dispersion has also

*E-mail: wangh586@mail.sysu.edu.cn; #Equally contributions

14th National Conference on Laser Technology and Optoelectronics (LTO 2019), edited by Jianqiang Zhu, Weibiao Chen, Zhenxi Zhang, Minlin Zhong, Pu Wang, Jianrong Qiu, Proc. of SPIE Vol. 11170, 111702H
© 2019 SPIE · CCC code: 0277-786X/19/$18 · doi: 10.1117/12.2533715

been achieved in recent work by correcting the chromatic aberration of metalenses to double wavelengths [21, 22], triple wavelength [23], and a continues wavelength range [24-27]. For some applications (e.g. two-photon fluorescence microscopy (TPM)) [28, 29], the optical elements with specific dispersion (zero, positive or negative) at double wavelength are attractive for compensating or expanding the dispersion of the entire optical system.

In this work, we proposed an alternative approach to engineer the chromatic dispersion in dual-wavelength metalenses. The inscribed-cross-shaped meta-atoms are designed to provide fully 2π phase coverages at the two discrete wavelengths independently. Three kinds of metalenses are demonstrated, including those with zero dispersion, positive axial dispersion, and negative axial dispersion. With the nearly diffractive-limited focusing, all metalenses operate in the transmission mode for the unpolorized light at 440 nm and 720 nm. Our results may pave a novel way for the double-wavelength functional applications in the fields of optical information processing, imaging technologies and complex fluorescence techniques.

2. PRINCIPLE

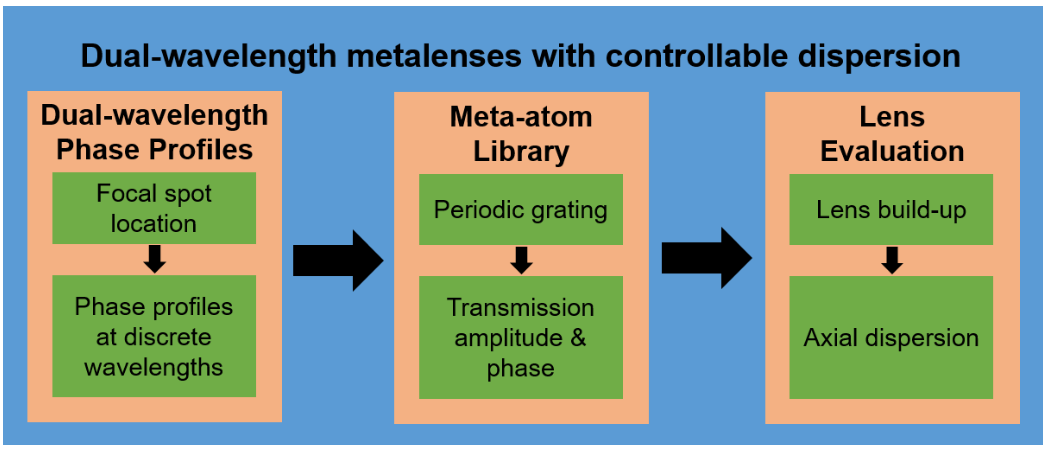

Figure 1. A schematic diagram shows the design process of dual-wavelength metalenses with controllable dispersion.

Figure 1 illustrates the design process of dual-wavelength metalenses with controllable dispersion. First, the design of dual-wavelength phase profiles is determined by the focal spot location according to the specific dispersion. A library is then built with a fruitful set of meta-atoms to fill as much as phase space at 440 nm and 720 nm. Finally, full wave simulation is done to derive the axial dispersion of the whole metalens.

Metasurfaces can almost achieve arbitrary phase, amplitude, polarization pixel by pixel. For our purposes, we only manipulate the phase for the normal incidence light. The total output phase Φ_{tot} through the metasurface propagation comes from two parts $\Phi_{tot}(x,y,\lambda)=\Phi_m(x,y,\lambda)+\Phi_p(x,y,\lambda)$, where Φ_m is the phase shift imparted by the metasurafe at the point (x,y) , and Φ_p is the uniform distribution phase via propagation in the homogeneous medium (i.e. the substrate). For a metalens, a spherical wavefront is guaranteed to focus the light and thus, for an arbitrary focal point with the spatial position $f_i=(x_i,y_i,z_i)$ at the wavelength of λ_i , the phase shift Φ_m can be designed as

$$\Phi_m(x,y,\lambda_i)=-\frac{2\pi}{\lambda_i}\left(\sqrt{\left(x-x_i\right)^2+\left(y-y_i\right)^2+z_i^{\,2}}-z_i\right) \quad (1),$$

where the subscript i is an integer. The dispersion of metalens can be defined as $\mathrm{s}=\mathrm{d}f/\mathrm{d}\lambda$, and for double wavelengths, we can use the difference form of $\mathrm{s}=\left(f_i-f_j\right)/\left(\lambda_i-\lambda_j\right)$. As the focal point relates to three-dimensional spatial position, the axial dispersion can be written as $\mathrm{s}_z=\left[f_i(z_i)-f_j(z_j)\right]/\left(\lambda_i-\lambda_j\right)$. To control the dispersion on a single-layer metalens at double wavelengths, the different focal points are required and can be set as two arbitrary spatial position. Hence, different phase profiles are needed at the designed wavelengths, according to the equation (1). For the demonstration of the design process, we have designed three kinds of metalenses with different dispersions at the wavelength of 440 nm and 720 nm. Note that the phase profiles at the different wavelengths should be decoupled. The phase modulations need to cover fully 2π range at both two wavelengths and the difference between them should take any value among 0-2π. In the following sections, we will show an approach to engineer the chromatic dispersion in dual-wavelength metalenses, in which the inscribed-cross-shaped meta-atoms are designed to provide fully 2π phase coverages at the two discrete wavelengths.

3. META-ATOM LIBRARY

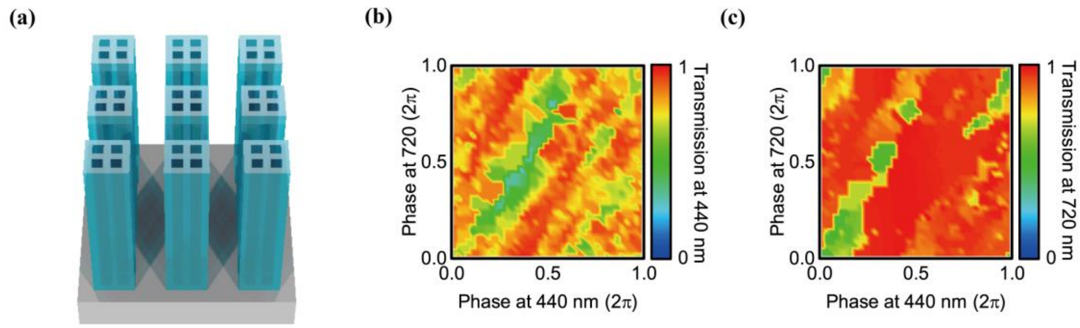

Figure 2. Meta-atom libraries. (a) Schematic drawing of meta-atoms, constructed by a silicon-rich nitride array (n = 2.4) with nanoposts on a fused silica substrate (n = 1.46). The square lattice constant is p = 420 nm, and the thickness of nanoposts is 1000 nm. (b), (c) Calculated transmittance of selected meta-atoms at 440 nm and 720 nm, respectively.

To realize the wavelength-independent phase modulations, we design a set of meta-atoms with fully 2π coverage at 440 nm and 720 nm in the periodic gratings. Various kinds of meta-atoms have been demonstrated by previous work, including gratings [11, 23], nanofins [17, 19], elliptical nanopillars [30], circular nanopillars [18] and composite nanopillars [24, 25]. Generally, such meta-atoms can be categorized by their polarization-dependence. In the pursuit of polarization-independent focusing, we choose the meta-atoms with four-fold symmetry to control the unpolarized light. In order to fill as much as phase space at 440 nm and 720 nm, we need to create the meta-library that contains a fruitful set of meta-atoms. As shown in Fig. 2(a), we consider the inscribed-cross-shaped pillars. It has been pointed out that the dispersion of meta-atoms comes from the interaction between light and the structures and materials, namely structural dispersion and material dispersion [31]. For simplicity, we neglect the material dispersion and regard the refractive index as a constant at the given double wavelengths. We perform the finite difference time domain (FDTD) method to simulate these gratings, yielding the phase and transmission at the wavelengths of interest. By the sweep algorithm, we have built a meta-atom library with over 10000 kinds of meta-atoms. Here, we consider the silicon-rich nitride (n = 2.4) as the material of meta-atoms and the substrate is silica (n = 1.46). The meta-atoms are then constructed to the periodic gratings, with the rectangular lattice constant of 420 nm and the height of 1000 nm.

For each desired combination of phases ϕ_1 at 440 nm and ϕ_2 at 720 nm, phase pairs $(\phi_1,\ \phi_2)$ can be implemented by the specific meta-atoms. To filter out the best meta-atoms, we take complex amplitude responds of meta-atoms into account, and use the transmission error [32, 33] of $\varepsilon = [\exp(i\phi_1) - t_1]^2 + [\exp(i\phi_2) - t_2]^2$, where t_1 and t_2 are the complex transmission coefficients at the two wavelengths. Finally, meta-atoms are filtered out from the meta-atom library by minimizing the transmission errors. The corresponding transmittances at 440 nm and 720 nm are also shown in Figs. 2(b) and 2(c), respectively.

4. DOUBLE-WAVELENGTH METALENSES WITH DIFFERENT DISPERSION

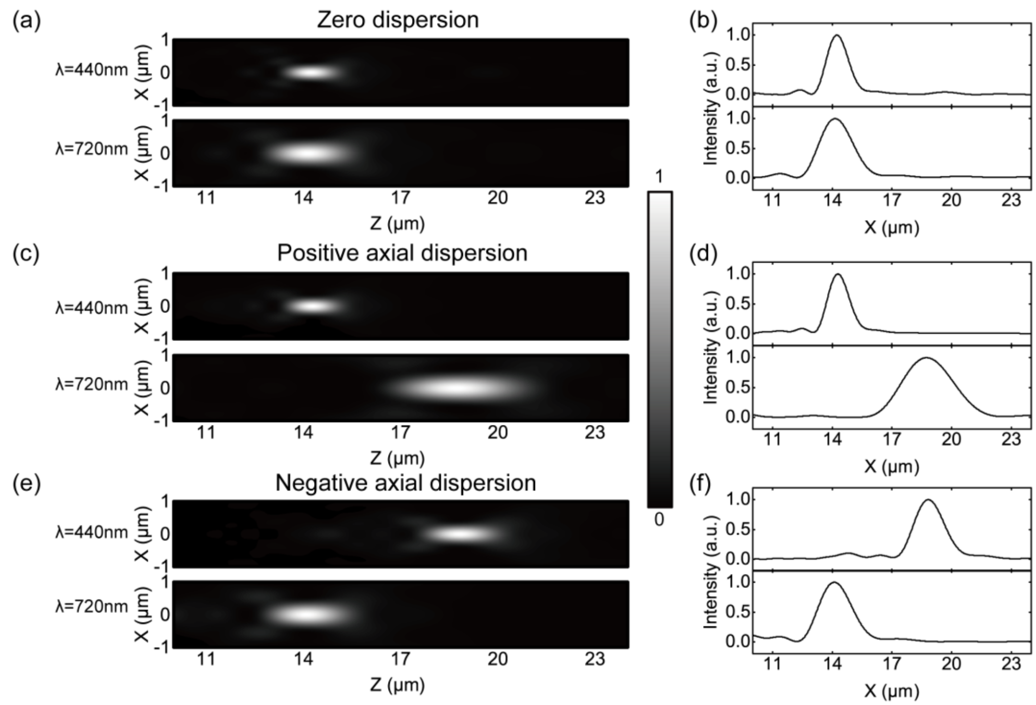

Figure 3. Comparison of different dispersion metalenses upon illumination with λ = 440 nm and 720 nm. (a) Normalized intensities distribution in xz-plane of zero dispersion metalens. (b) Corresponding cross sections in z direction through the center of the focal spots. (c)-(f) Similar results to (a)-(b), but for positive and negative axial dispersion metalenses.

With the above-mentioned meta-atoms, the double-wavelength metalenses with arbitrary dispersions can be realized theoretically. We first show a 30-μm-diameter metalens with zero dispersion that axial dispersion is equal to zero ($s_z = 0$) at 440 nm and 720 nm, focusing the light at a distance of 14 μm on the same position behind the metalens, yielding the corresponding numerical aperture (NA) as large as 0.73. Figure 3(a) gives the simulated results of the normalized intensity distributions in xz-plane across the focal spots. It is obvious that only one focus in the output field at each wavelength and the simulations greatly verify the feasibility of our designs with the focal lengths of 14.2 μm at both two wavelengths. The corresponding cuts of the focal spots along z are plotted in Fig. 3(b). The simulated full-widths at half-maximums (FWHMs) are 325 and 510 nm at the wavelength of 440 nm and 720 nm respectively, close to the diffraction-limited values (301 nm at 440 nm, 493 nm at 720 nm). To characterize the focusing property of such zero dispersion metalens, we further calculate the focusing efficiencies of 18.68% at 440 nm and 54.74% at 720 nm, by extracting the optical power ratio of the focal spot to the incident beam.

To describe the flexibility of our proposed method, we also design two metalenses of equal size but with different axial dispersion, one is positive and another is negative. The positive one focuses the purple light (440 nm) to the distance of 14 μm and the red light (720 nm) to 19 μm, yielding the axial dispersion of $s_z \approx 17.9$ nm/nm. In contrast, the negative one has the focal length of 19 μm at 440 nm and 14 μm at 720 nm, yielding the opposite axial dispersion of $s_z \approx -17.9$ nm/nm. The normalized intensity distribution of the positive axial dispersion metalens in xz-plane are shown in Fig. 3(c) while the negative one in Fig. 3(e). Figure 3(d) plots the relevant cross sections in the z direction respectively, and the similar results for the negative one are plotted in Fig. 3(f). Note that the results show the axial dispersion of $s_z \approx 15.9$ nm/nm in the positive axial dispersion metalens with the focal lengths of 14.28 μm at 440 nm and 18.74 μm at 720 nm, approximate consistence of the designed parameters. For the negative one, the simulated axial dispersion is $s_z \approx -16.9$ nm/nm, with the focal lengths of 18.82 μm at 440 nm and 14.10 μm at 720 nm, respectively. Hence, the analysis results in both two metalenses are well consistent with our theoretical designs. We also calculate the normalized intensities in the x direction of the focal spots in both metalenses. The FWHMs are 345 nm (with 19.60% efficiency at

440 nm) and 571 nm (with 42.02% at 720 nm) in the positive axial dispersion metalens, comparable to the diffraction-limited FWHMs (301 nm at 440 nm and 493 nm at 720 nm). In the negative one, the purple light has the FWHM of 395 nm (with 22.71% efficiency) and red light is 511 nm (with 50.69%), also close to the diffraction limits (355 nm at 440 nm and 493 nm at 720 nm).

5. CONCLUSION

In conclusion, we have proposed a versatile method to engineer the chromatic dispersion in double-wavelength metalenses in the visible region. In particular, the polarization-independent meta-atoms are presented to realize the two phase profiles at the wavelengths of interest independently. As a proof of concept, three metalenses with different dispersion are reported, including zero dispersion metalens, positive axial dispersion metalens, and negative axial dispersion metalens. All metalenses demonstrate the high resolution powers with the nearly diffraction-limited focusing properties. Finally, our findings may open new avenues for the wavelength-controlled multifunctional applications, including optical information encryption, imaging technologies and complex fluorescence imaging techniques.

ACKNOWLEDGEMENTS

This work is supported by the National Natural Science Foundation of China (No. 61775243, No. 11761161002, No. 11704422), Natural Science Foundation of Guangdong Province (No. 2018B030308005), Science and Technology Program of Guangzhou (No. 201804020029).

REFERENCES

[1] J. F. James, R. S. Sternberg, and S. A. Rice, "The design of optical spectrometers," Physics Today, 23, 55 (1970).

[2] H. Kosaka, T. Kawashima, A. Tomita et al., "Superprism phenomena in photonic crystals," Physical review B, 58(16), R10096 (1998).

[3] V. Huet, A. Rasoloniaina, P. Guillemé et al., "Millisecond photon lifetime in a slow-light microcavity," Physical review letters, 116(13), 133902 (2016).

[4] A. Szulc, "Improved solution for the cemented doublet," Applied optics, 35(19), 3548-3558 (1996).

[5] R. D. Blakley, "Dialyte-refractor design for self-correcting lateral color," Optical Engineering, 42(2), 400-405 (2003).

[6] P. Hariharan, "Apochromatic lens combinations: A novel design approach," Optics Laser Technology, 29(4), 217-219 (1997).

[7] J. Reimers, A. Bauer, K. P. Thompson et al., "Freeform spectrometer enabling increased compactness," Light: Science and Applications, 6(7), e17026 (2017).

[8] N. Yu, P. Genevet, M. A. Kats et al., "Light propagation with phase discontinuities: generalized laws of reflection and refraction," Science, 334(6054), 333-337 (2011).

[9] A. V. Kildishev, A. Boltasseva, and V. M. Shalaev, "Planar photonics with metasurfaces," Science, 339(6125), 1232009 (2013).

[10] H.-T. Chen, A. J. Taylor, and N. Yu, "A review of metasurfaces: physics and applications," Reports on progress in physics, 79(7), 076401 (2016).

[11] D. Sell, J. Yang, S. Doshay et al., "Large-angle, multifunctional metagratings based on freeform multimode geometries," Nano letters, 17(6), 3752-3757 (2017).

[12] X. Ni, N. K. Emani, A. V. Kildishev et al., "Broadband light bending with plasmonic nanoantennas," Science, 335(6067), 427-427 (2012).

[13] R. C. Devlin, A. Ambrosio, N. A. Rubin et al., "Arbitrary spin-to–orbital angular momentum conversion of light," Science, 358(6365), 896-901 (2017).

[14] B. Wang, F. Dong, Q.-T. Li et al., "Visible-frequency dielectric metasurfaces for multiwavelength achromatic and highly dispersive holograms," Nano letters, 16(8), 5235-5240 (2016).

[15] Z.-L. Deng, and G. Li, "Metasurface optical holography," Materials Today Physics, 3, 16-32 (2017).

[16] S. Kruk, B. Hopkins, I. I. Kravchenko et al., "Invited Article: Broadband highly efficient dielectric metadevices

for polarization control," Apl Photonics, 1(3), 030801 (2016).
[17] M. Khorasaninejad, W. T. Chen, R. C. Devlin et al., "Metalenses at visible wavelengths: Diffraction-limited focusing and subwavelength resolution imaging," Science, 352(6290), 1190-1194 (2016).
[18] Z.-B. Fan, Z.-K. Shao, M.-Y. Xie et al., "Silicon nitride metalenses for close-to-one numerical aperture and wide-angle visible imaging," Physical Review Applied, 10(1), 014005 (2018).
[19] A. Y. Zhu, W.-T. Chen, M. Khorasaninejad et al., "Ultra-compact visible chiral spectrometer with meta-lenses," Apl Photonics, 2(3), 036103 (2017).
[20] M. Khorasaninejad, W. T. Chen, J. Oh et al., "Super-dispersive off-axis meta-lenses for compact high resolution spectroscopy," Nano letters, 16(6), 3732-3737 (2016).
[21] J. Yan, Y. Guo, M. Pu et al., "High-efficiency multi-wavelength metasurface with complete independent phase control," Chinese Optics Letters, 16(5), 050003 (2018).
[22] E. Arbabi, J. Li, R. J. Hutchins et al., "Two-photon microscopy with a double-wavelength metasurface objective lens," Nano letters, 18(8), 4943-4948 (2018).
[23] M. Khorasaninejad, F. Aieta, P. Kanhaiya et al., "Achromatic metasurface lens at telecommunication wavelengths," Nano letters, 15(8), 5358-5362 (2015).
[24] S. Shrestha, A. C. Overvig, M. Lu et al., "Broadband achromatic dielectric metalenses," Light: Science and Applications 7(1), 85 (2018).
[25] W. T. Chen, A. Y. Zhu, J. Sisler et al., "Broadband achromatic metasurface-refractive optics," Nano letters, 18(12), 7801-7808 (2018).
[26] W. T. Chen, A. Y. Zhu, V. Sanjeev et al., "A broadband achromatic metalens for focusing and imaging in the visible," Nature nanotechnology, 13(3), 220 (2018).
[27] S. Wang, P. C. Wu, V.-C. Su et al., "Broadband achromatic optical metasurface devices," Nature communications, 8(1), 187 (2017).
[28] F. Helmchen, and W. Denk, "Deep tissue two-photon microscopy," Nature methods, 2(12), 932 (2005).
[29] W. Denk, J. H. Strickler, and W. W. Webb, "Two-photon laser scanning fluorescence microscopy," Science, 248(4951), 73-76 (1990).
[30] E. Arbabi, A. Arbabi, S. M. Kamali et al., "High efficiency double-wavelength dielectric metasurface lenses with dichroic birefringent meta-atoms," Optics Express, 24(16), 18468-18477 (2016).
[31] X. Li, M. Pu, X. Ma et al., "Dispersion engineering in metamaterials and metasurfaces," Journal of Physics D: Applied Physics, 51(5), 054002 (2018).
[32] Z. Shi, M. Khorasaninejad, Y.-W. Huang et al., "Single-layer metasurface with controllable multiwavelength functions," Nano letters, 18(4), 2420-2427 (2018).
[33] E. Arbabi, A. Arbabi, S. M. Kamali et al., "Multiwavelength polarization-insensitive lenses based on dielectric metasurfaces with meta-molecules," Optica, 3(6), 628-633 (2016).